Effect of dimensionality on sliding charge density waves: The quasi-two-dimensional $TbTe_3$ system probed by coherent x-ray diffraction

D. Le Bolloc'h,[1] A. A. Sinchenko,[2] V. L. R. Jacques,[1] L. Ortega,[1] J. E. Lorenzo,[3] G. A. Chahine,[4] P. Lejay,[3] and P. Monceau[3]

[1]*Laboratoire de Physique des Solides, CNRS, Univ. Paris-Sud, Université Paris-Saclay, 91405 Orsay, France*

[2]*Kotel'nikov Institute of Radioengineering and Electronics of RAS, Mokhovaya 11-7, 125009 Moscow, Russia*

[3]*Institute Néel, CNRS and Université Grenoble-Alpes, BP166, 38042 Grenoble, France*

[4]*ESRF, 71 avenue des Martyrs, 38000 Grenoble, France*

(Received 24 June 2015; revised manuscript received 2 February 2016; published 18 April 2016)

We report on sliding charge density waves (CDWs) in the quasi-two-dimensional $TbTe_3$ system probed by coherent x-ray diffraction combined with *in situ* transport measurements. We show that the non-Ohmic conductivity in $TbTe_3$ is made possible thanks to a strong distortion of the CDW. Our diffraction experiment versus current shows first that the CDW remains undeformed below the threshold current I_S and then suddenly rotates and reorders by motion above threshold. Contrary to quasi-one-dimensional systems, the CDW in $TbTe_3$ does not display any phase shifts below I_S and tolerates only slow spatial variations of the phase above. This is the first observation of CDW behavior in the bulk in a quasi-two-dimensional system allowing collective transport of charges at room temperature.

DOI: 10.1103/PhysRevB.93.165124

The interaction between pairs of quasiparticles often leads to broken-symmetry ground states in solids. Typical examples are the formation of Cooper pairs in superconductors, charge density waves (CDWs), and spin density waves driven by electron-phonon or electron-electron interactions [1]. The CDW ground state is characterized by a spatial modulation $\eta\cos(2k_F x+\phi)$ of the electron density and a concomitant periodic lattice distortion with the same $2k_F$ wave vector leading to a gap opening in the electron spectrum.

The first CDW systems were discovered in the beginning of the 70s in two-dimensional transition-metal dichalcogenides MX_2 [2]. The CDW state was then discovered in quasi-one-dimensional systems like $NbSe_3$, TaS_3, the blue bronze $K_{0.3}MoO_3$, and in organic compounds like TTF-TNCQ. However, the most remarkable property of a CDW was discovered a few years later in quasi-one-dimensional systems: a CDW may *slide* carrying correlated charges [3]. The sliding mode is achieved when an electric field applied to the sample is larger than a threshold value, manifesting then collective Fröhlich-type transport. This sliding phenomenon is clearly observed by transport measurements. The differential resistance remains constant up to a threshold current and then decreases for larger currents in addition to the generation of an ac voltage, the frequency of which increases with the applied current [3].

In spite of numerous studies, the physical mechanism leading to the sliding phenomenon is still far from being fully understood. One of the difficulties comes from the fact that the sliding mode displays two different aspects. On the one hand, the CDW is a classical state, similar to an elastic object in presence of disorder [4], displaying creep, memory effects, and hysteresis [5,6]. On the other hand, a CDW is a macroscopic quantum state [7], carrying charges by tunneling through disorder [8] and displaying Aharonov–Bohm effects [9] over microscopic distances [10].

Recently, a new class of quasi-two-dimensional CDW compounds, rare-earth tritellurides RTe_3, have raised an intense research activity thanks to their peculiar properties [11–13]. RTe_3 structures are orthorhombic (*Cmcm*), but the a and c lattice parameters lying in the Te planes are almost equal ($c-a=0.002$ Å with $a=4.307$ Å for $TbTe_3$ at $T=300$ K) and the double Te layers are linked together by a c-glide plane. The almost-square Te sheets lead to nearly isotropic properties in the (a,c) plane. The resistance measured along a and c differs by only 10% at 300 K in $TbTe_3$ [14] and the Fermi surface displays an almost-square closed shape in the (a^*,c^*) plane [15]. These quasi-two-dimensional systems exhibit a unidirectional CDW wave vector along c^* ($2k_F\sim 2/7c^*$ in $TbTe_3$) and a surprisingly large Peierls transition temperature, around 300 K, through the whole R series and above for lighter rare-earth elements. The stabilization of the CDW in $TbTe_3$ over the almost-square underlying atomic lattice is reminiscent of copper-oxide planes in high-temperature superconductors in which a CDW state was also recently observed [16].

However, the most surprising property of $TbTe_3$ is its ability to display nonlinear transport [17] despite the two-dimensional character of the atomic structure. The aim of the present work is to show that, despite similar resistivity curves, the depinning process in quasi-one- and quasi-two-dimensional systems are quite different. For that purpose, coherent x-ray diffraction has been used to study the behavior of the $2k_F$ satellite reflection upon application of an external current.

Because the sliding state of a CDW mainly involves fluctuations of the CDW phase to overcome pinning centers, coherent x-ray diffraction is a suitable technique thanks to its high sensitivity to the phase of any modulation. The extreme case of a single phase shift, such as a dislocation, can locally induce the disappearance of Bragg peaks while a single topological defect is very difficult or impossible to detect with conventional x-ray beams [18]. This approach enabled us to highlight a dislocation of the CDW [19] and an regular array of CDW dislocations [20]. Thanks to the high brilliance of synchrotron sources and improved optics, coherent x-ray beams, tens of micrometers in size, can be obtained with coherence properties very similar to those of lasers [21]. The experiment described herein was performed at the ID01 beam line of the European Synchrotron Radiation Facility

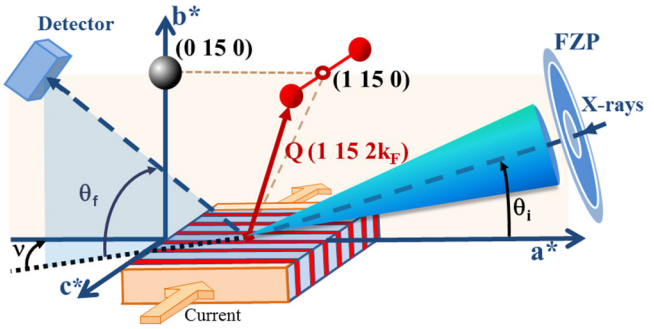

FIG. 1. Experimental diffraction setup (not to scale) with a coherent $0.5 \times 0.5\ \mu m^2$ focused x-ray spot. The $(1\ 15\ 2k_F)$ CDW satellite reflection, associated with the (1 15 0) Bragg (forbidden) reflection, was probed with a 2D detector mounted on a lifting detector arm.

(ESRF). A channel-cut Si(111) monochromator was used with a longitudinal coherence length $\xi_L = \lambda^2/2\Delta\lambda = 0.6\ \mu m$ at $E = 7.4$ keV ($\lambda = 1.675$ Å). At this energy, the penetration length of the x-ray beam is $\mu^{-1} \approx 4\ \mu m$ allowing us to probe the sample volume. The optical path was defined by a slit opened at $S_0 = 20(H) \times 60(V)\ \mu m^2$ at 40 cm from the sample, followed by a Fresnel zone plate that focused the coherent x-ray beam down to $0.5\ \mu m \times 0.5\ \mu m$, 23 cm further on the sample. The two-dimensional (2D) diffraction patterns were recorded with a pixel detector ($55\ \mu m \times 55\ \mu m$ pixels size) and located 1.2 m from the sample.

A slightly modified method like the one described in Ref. [23] was used to grow high-quality $TbTe_3$ crystals. A 1 mm^2 square sample, 1.6 μm thick, was then selected and cleaved to obtain an elongated shape (1 mm long and 120 μm wide). The c^* orientation was checked by diffraction thanks to the reflection conditions of the *Cmcm* space group: $(0, k\ l)$, $k = 2n$ and $(h\ 0\ l)$, $h,l = 2n$. A four-contact method was used for transport measurements with 0.6 mm between the two inner contacts. The resistance ratio between room and helium temperature was typically larger than 100, similar to previous reports [12]. The current-voltage curve was regularly measured during the experiment, showing a very stable threshold current $I_S = 11$ mA [Fig. 2(d)]. The threshold remained stable during several days of experiment, suggesting no radiation damage by x-rays. This indication is reinforced by the remarkable stability of the $2k_F$ satellite intensity and of the resistance during acquisitions. This is an important difference with quasi-one-dimensional systems such as $NbSe_3$ and $K_{0.3}MoO_3$ in which the CDW is irreversibly damaged by excessively intense x-ray beams.

The $Q(1\ 15\ 2k_F)$ satellite reflection associated with the CDW was measured in reflection geometry at room temperature (see setup in Fig. 1 with $\theta_i \approx 11°$, $\theta_f = 63.8°$ and $\nu = 12.9°$). A micrometer $0.5\ \mu m \times 0.5\ \mu m$ coherent beam was used, focused with Fresnel zone plates (FZPs). In the pristine state, without external current, the sample displays a transverse CDW correlation lengths of $\xi_T \approx 40$ nm [obtained from the main peak of the rocking curve in Fig. 2(b)]. The rocking curve of the $2k_F$ satellite displays also a second contribution from a disoriented domain, three times weaker in intensity [see the arrow in Figs. 2(b) and 3(a)]. The coherent

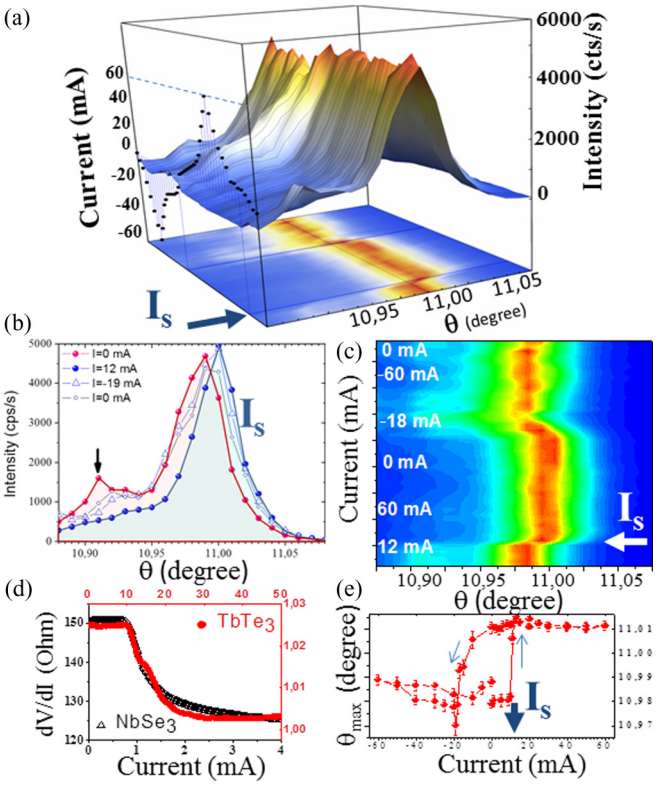

FIG. 2. (a) Rocking curve of the $Q = (1\ 15\ 2k_F)$ satellite reflection associated with the CDW in $TbTe_3$ versus external current at $T = 300$ K. The intensity was integrated over the whole pixel camera. The left panel shows the corresponding currents applied to the sample. (b) Intensity profile of the $Q = (1\ 15\ 2k_F)$ satellite reflection for several currents showing the shifted profile at I_S in blue and (c) the corresponding $2k_F$ profile versus current. (d) Differential resistance measured *in situ* during the x-ray experiment in $TbTe_3$ (red dots) and in $NbSe_3$ (black triangles from Ref. [22]) with $I_S = 11$ mA for $TbTe_3$. (e) Main satellite position versus current showing a large hysteresis (a Lorentzian profile is used to fit the main peak).

diffraction pattern displays many speckles distributed almost isotropically and coming from CDW phase shifts in the $(\mathbf{a}^*,\mathbf{c}^*)$ plane and between sheets along $\mathbf{b}^*$ direction [see Fig. 3(a)].

The scattering features of the $Q(1\ 15\ 2k_F)$ satellite reflection were studied with respect to applied currents, both below and above the threshold current ($I_S = 11$ mA). Typical excursion ranged from $I = 0$ mA up to 60 mA and then back to $I = 0$ mA [see Figs. 2(a) and 2(c)]. The increase of current from $I = 0$ mA to below the threshold current hardly changes the diffraction pattern. The distribution of speckles does not change although slight variations in intensity are observed [see Fig. 3(a)].

At I_S, a drop of 2% of the differential resistance is measured and the satellite reflection changes. The satellite's position increases by 0.013° in θ [see blue curve in Fig. 2(b)], the width of the main peak decreases, its intensity increases slightly and the small contribution coming from the disoriented domain disappears. Just above the threshold current, an increase of 14% of the transverse CDW correlation length ξ_T is observed. The isotropic diffraction pattern remains but the distribution

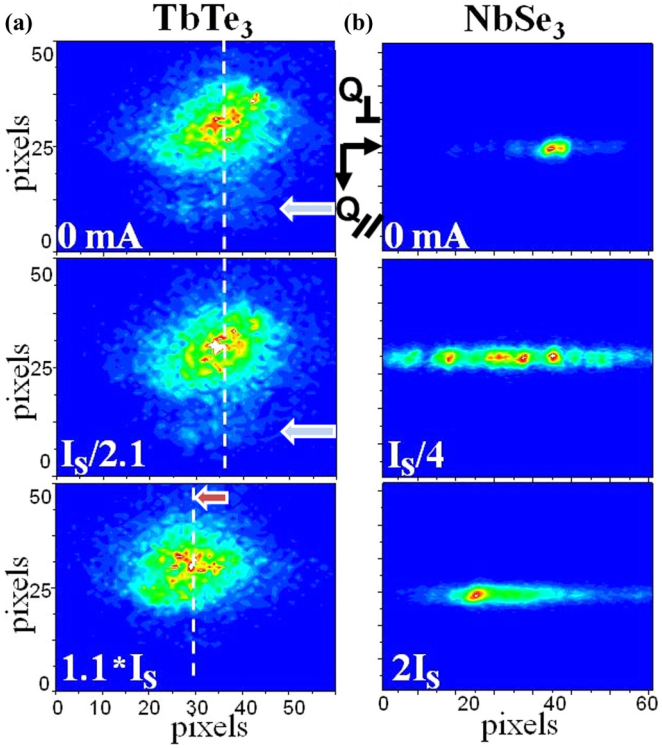

FIG. 3. Coherent diffraction patterns of the $2k_F$ satellite reflection associated with the CDW versus external current, below and above the threshold current I_S, in (a) the quasi-two-dimensional $TbTe_3$ system (for $I = 0$ mA, $I = I_S/2.1 = 5$ mA and $I = 1.1I_S = 12$ mA at $T = 300$ K) and (b) in the quasi-one dimensional $NbSe_3$ system (from Ref. [22]) at $T = 120$ K. The 2D images are a sum over several θ angles through the maximum of intensity. For $TbTe_3$, the blue arrow indicates the contribution of the disoriented domain contributing in the profile in Fig. 2(b) and the red one indicates the shift of the $2k_F$ reflection at I_S. Although the cutting plane is different in the two cases, the vertical direction of the camera is close to the $2k_F$ wave vector ($Q_\parallel$) and the horizontal one is transverse to $2k_F$ ($Q_\perp$) in both cases.

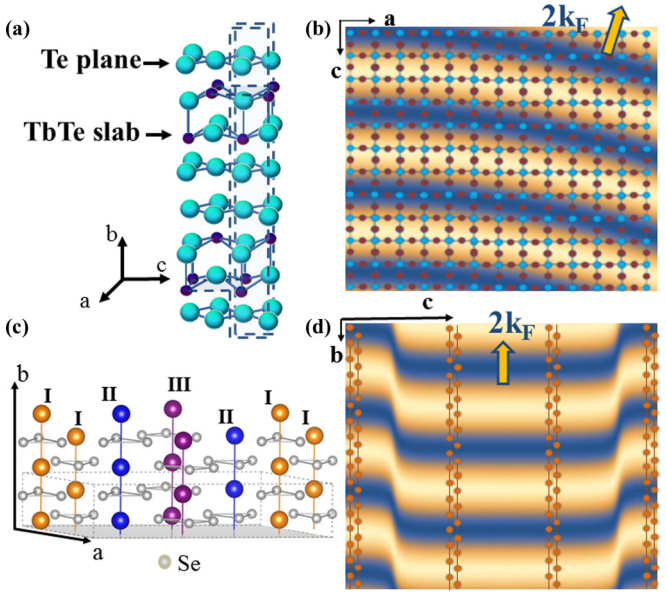

FIG. 4. (a) Sketch of the $TbTe_3$ structure and (b) its projection along b in the (a,c) plane. (c) $NbSe_3$ structure with the three types of chains (only the first chain, the orange one, participates in the q_1 CDW) and (d) projection of chains I along a in the (b,c) plane. In both systems, the CDW is represented by blue wavefronts in panels (b) and (d).

of speckles is totally different. The CDW reorders above I_S but also rotates by an angle $\beta = 0.02^\circ$ [see the red arrow in Fig. 3(a)] with a complete reorganization of domains.

The rotation of the wave vector is clearly observed when using a very small 0.5 μm beam. When the measurement is performed with a 100-times larger beam (without focusing with the FZP), averaging over a 100^2-times larger volume, the $2k_F$ rotation is still observed but significantly less pronounced. Increasing the spatial average blurs the signature by including contributions of smaller domains.

The CDW behavior versus current is almost reversible but with a strong hysteresis [see Fig. 2(e)]. The gradual increase in current from $I > I_S$ to $I = 5.45I_S = 60$ mA induces almost no change compared to the state just above the threshold current. The satellite remains also unchanged when decreasing current down to $I = 0$ mA and even further down to negative currents. Only at $I = -19$ mA does the satellite resume its original state. Back to $I = 0$ mA, finally, the $2k_F$ profile is close to the initial state, but not identical; however, with a larger width and smaller intensity. The contribution from the small disoriented domain also reappears [see Fig. 2(b)]. All these observations show that the distorted CDW state is a frozen metastable state which can be released by reversing the applied current.

The experiment was repeated several times. When changing the beam position on the sample, the CDW displays similar features, including rotation and narrowing. However the rotation direction and its amplitude may change. The fundamental Bragg peaks q_0 does not depend on current (within our resolution) excluding any thermal effect induced by external currents.

This measurement first demonstrates that the CDW deformation is directly involved in the nonlinear transport observed in $TbTe_3$. The sliding state is reached thanks to a rotation of the $2k_F$ wave vector to overcome pinning centers and a reordering of the CDW by motion. This rotation versus current is almost reversible and strongly hysteretic. Motional narrowing and hysteresis are common features with quasi-one-dimensional systems such as $NbSe_3$ [22] and $K_{0.3}MoO_3$ [20,24].

However, the two types of systems widely differ from each other by the type of CDW distortions. Contrary to $TbTe_3$, $NbSe_3$ displays creep for currents well below the threshold. This corresponds to the presence of speckles along a line in the reciprocal lattice [see Fig. 3(b)] due to abrupt CDW phase shifts parallel to the chain axis in real space [see Fig. 4(d)] [22]. Rotation of the $2k_F$ wave vector is not observed in $NbSe_3$ while creep is not observed in $TbTe_3$.

This difference in behavior is mainly explained by the difference in dimensionality of the two systems. Contrary to the quasi-two-dimensional $TbTe_3$ system, $NbSe_3$ is quasi-one dimensional, made of parallel chains of atoms along which the resistance and the elastic constants are at least ten times smaller than in the two other perpendicular directions. $TbTe_3$

displays an almost-square Fermi surface, while $NbSe_3$ displays an open Fermi surface, consisting of two nearly parallel planar surfaces perpendicular to the atomic chains [25].

The $TbTe_3$ behavior above I_S can be explained by elastic theory, considering the CDW as an incompressible lamellar phase in the presence of disorder. This phenomenon is linked to a shear of the CDW which can be treated by considering a spatial dependence of the phase $\Phi(x,y)$, where x is the direction parallel to $2k_F$ and y is the transverse direction [4]. Transverse deformations such as shears, which do not compress or dilate the CDW modulation, are neutral and will be favored. In the framework of elastic theory, the equilibrium state fulfilled the equation $k_t \frac{\partial^2 \Phi}{\partial^2 y} = qE$ where k_t is the elastic constant along the transverse axis and E is the applied field.

In $TbTe_3$, the underlying lattice seen by the CDW is almost homogeneous and k_t can be considered constant in space. Taking into account the boundary conditions $[\Phi(0) = \Phi(l) = 0]$, the solution to the previous equation is a parabolic function in y: $\Phi(y) \propto y(l-y)$, where l is a macroscopic distance corresponding to distances between strong pinning centers, side edges, or surface steps. Thus $\Phi(y)$ slowly varies with space, inducing a smooth rotation of the $2k_F$ wave vector as shown in Fig. 4(b), in agreement with our measurement. This loss of orientational symmetry of the CDW compared with the atomic lattice recalls disclinations found in smectic liquid crystals due to pinning at surfaces, where incompressibility is due to steric issues in that case [26].

In $NbSe_3$, only one type of Nb chain out of three is involved in the q_1 CDW [called chains I in orange in the structure displayed in Fig. 4(c)]. Since more than 15.6 Å separates two groups of chains I, the effective elastic constant strongly varies along the transverse direction and the continuous elastic model used for $TbTe_3$ is not appropriate anymore. This strong structural anisotropy leads to abrupt CDW phase shifts, as illustrated in Fig. 4(d) (without compressing or expanding CD wavefronts). In that case, speckles appear along a line, without tilt, in agreement with our measurement.

Below threshold, the two systems also display a very different behavior. At low currents, the strong deformation of the CDW in $NbSe_3$ is not observed in $TbTe_3$ in which the diffraction pattern remains nearly identical to the same distribution of speckles up to I_S. Contrary to $NbSe_3$ and $K_{0.3}MoO_3$, which both display the creep phenomenon, the homogeneity of the $TbTe_3$ atomic lattice seems to prohibit all types of CD wavefront deformation below I_S, suggesting a strong pinning scenario [27] due to dimensionality.

At I_S, the CDW abruptly depins, as expected from strong-pinning theory [28], where the phase adjusts locally around each pinning center for $I < I_S$. Note that the sudden collective depinning at I_S, measured by diffraction which probes submicrometer domains, is totally correlated with transport measurements averaging over the 0.6 mm gap between the two electrodes. In the sliding state however, only slow spatial variations of the phase are observed, suggesting a collective deformation of the phase over large distances. This sudden CDW deformation at the threshold current, without creep below threshold, may be related to the strong electron-phonon coupling invoked to explain the offset of the wave vector of Fermi surface nesting relative to the $2k_F$ observed in $TbTe_3$ [29].

[1] G. Grüner, *Density Waves in Solids* (Addison-Wesley, Reading, 1994); L. Gorkov and G. Grüner, *Charge Density Waves in Solids* (Elsevier Science, Amsterdam, 1989); *Electronic Crystals* 2011, edited by S. Brazovskii, N. Kirova, and P. Monceau, Phys. B (Amsterdam, Neth.) **407**, 1683 (2012).

[2] For a review see A. Wilson, F. J. DiSalvo, and S. Mahajan, Adv. Phys. **24**, 117 (1975).

[3] For a recent review see P. Monceau, Adv. Phys. **61**, 325 (2012).

[4] D. Feinberg and J. Friedel, in *Low-Dimensional Electronic Properties of Molybdenum Bronzes and Oxides*, edited by C. Schlenker (Klüwer Academic, Dordrecht, 1989), p 407; J. Phys. (Paris) **49**, 485 (1988).

[5] S. Brazovskii and T. Nattermann, Adv. Phys. **53**, 177 (2004).

[6] T. Giamarchi and P. Le Doussal, Phys. Rev. Lett. **76**, 3408 (1996).

[7] J. Bardeen, Phys. Rev. Lett. **42**, 1498 (1979).

[8] T. L. Adelman, S. V. Zaitsev-Zotov, and R. E. Thorne, Phys. Rev. Lett. **74**, 5264 (1995).

[9] Y. I. Latyshev, O. Laborde, P. Monceau, and S. Klaumunzer, Phys. Rev. Lett. **78**, 919 (1997).

[10] M. Tsubota, K. Inagaki, T. Matsuura, and S. Tanda, Europhys. Lett. **97**, 57011 (2012).

[11] E. DiMasi, M. C. Aronson, J. F. Mansfield, B. Foran, and S. Lee, Phys. Rev. B **52**, 14516 (1995).

[12] N. Ru, J.-H. Chu, and I. R. Fisher, Phys. Rev. B **78**, 012410 (2008); N. Ru, C. L. Condron, G. Y. Margulis, K. Y. Shin, J. Laverock, S. B. Dugdale, M. F. Toney, and I. R. Fisher, *ibid.* **77**, 035114 (2008).

[13] G.-H. Gweon, J. D. Denlinger, J. A. Clack, J. W. Allen, C. G. Olson, E. D. DiMasi, M. C. Aronson, B. Foran, and S. Lee, Phys. Rev. Lett. **81**, 886 (1998).

[14] A. A. Sinchenko, P. D. Grigoriev, P. Lejay, and P. Monceau, Phys. Rev. Lett. **112**, 036601 (2014).

[15] V. Brouet, W. L. Yang, X. J. Zhou, Z. Hussain, R. G. Moore, R. He, D. H. Lu, Z. X. Shen, J. Laverock, S. B. Dugdale, N. Ru, and I. R. Fisher, Phys. Rev. B **77**, 235104 (2008).

[16] G. Ghiringhelli, M. Le Tacon, M. Minola, S. Blanco-Canosa, C. Mazzoli, Science **337**, 821 (2012); T. Wu *et al.*, Nature (London) **191**, 4 (2011); D. Le Boeuf, S. Krämer, W. N. Hardy, R. Liang, D. A. Bonn, and C. Proust, Nat. Phys. **9**, 79 (2013).

[17] A. A. Sinchenko, P. Lejay, O. Leynaud and P. Monceau, Solid State Comm. **188**, 67 (2014).

[18] V. L. R. Jacques, S. Ravy, D. Le Bolloc'h, E. Pinsolle, M. Sauvage-Simkin, and F. Livet, Phys. Rev. Lett. **106**, 065502 (2011).

[19] D. Le Bolloc'h, S. Ravy, J. Dumas, J. Marcus, F. Livet, C. Detlefs, F. Yakhou, and L. Paolasini, Phys. Rev. Lett. **95**, 116401 (2005).

[20] D. Le Bolloc'h, V. L. R. Jacques, N. Kirova, J. Dumas, S. Ravy, J. Marcus, and F. Livet, Phys. Rev. Lett. **100**, 096403 (2008).
[21] V. L. R. Jacques, D. Le Bolloc'h, E. Pinsolle, F. E. Picca, and S. Ravy, Phys. Rev. B **86**, 144117 (2012).
[22] E. Pinsolle, N. Kirova, V. L. R. Jacques, A. A. Sinchenko, and D. Le Bolloc'h, Phys. Rev. Lett. **109**, 256402 (2012).
[23] N. Ru and I. R. Fisher, Phys. Rev. B **73**, 033101 (2006).
[24] V. L. R. Jacques, D. Le Bolloc'h, S. Ravy, J. Dumas, C. V. Colin, and C. Mazzoli, Phys. Rev. B **85**, 035113 (2012).
[25] J. Schäfer, E. Rotenberg, S. D. Kevan, P. Blaha, R. Claessen, and R. E. Thorne, Phys. Rev. Lett. **87**, 196403 (2001); J. Schäfer, M. Sing, R. Claessen, Eli Rotenberg, X. J. Zhou, R. E. Thorne, and S. D. Kevan, *ibid.* **91**, 066401 (2003); H. Ando, T. Yokoya, K. Ishizaka, St. Suda, T. Kiss, S. Shin, T. Eguchi, M. Nohara and H. Takagi, J. Phys.: Condens. Matter **17**, 4935 (2005).
[26] M. Kleman, Rep. Prog. Phys. **52**, 555 (1989).
[27] H. Fukuyama and P. A. Lee, Phys. Rev. B **17**, 535 (1978).
[28] J. R. Tucker, W. G. Lyons, and G. Gammie, Phys. Rev. B **38**, 1148 (1988).
[29] M. Maschek, S. Rosenkranz, R. Heid, A. H. Said, P. Giraldo-Gallo, and I. R. Fisher, and F. Weber, Phys. Rev. B **91**, 235146 (2015).